Heliyon 9 (2023) e20163

Contents lists available at ScienceDirect

Heliyon

journal homepage: www.cell.com/heliyon

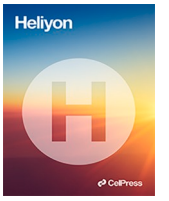

# Curcumin reverses erastin-induced chondrocyte ferroptosis by upregulating Nrf2

Yizhao Zhou **, Zhen Jia, Jing Wang, Shu Huang, Shu Yang, Sheng Xiao, Duo Xia, Yi Zhou *

*Department of Orthopedics, Hunan Provincial People's Hospital, The First-Affiliated Hospital of Hunan Normal University, Changsha, 410005, China*

ARTICLE INFO

*Keywords:*
Osteoarthritis
Ferroptosis
Curcumin
Nrf2
Erastin

ABSTRACT

Osteoarthritis (OA) is associated with ferroptosis, a newly discovered form of programmed cell death associated with lipid peroxidation. Curcumin, the main monomer component in turmeric rhizomes, possesses antioxidant and anti-ferroptosis properties, but its effect on ferroptosis in chondrocytes of OA is unknown. This study aimed to investigate the protective effect and potential mechanism of curcumin on chondrocytes induced by erastin, a ferroptosis inducer. CCK-8 assays were used to assess cell viability in mouse primary chondrocytes treated with 3.33 μM erastin alone or in combination with different doses of curcumin. Various parameters were detected, including LDH, SOD, GSH-PX, MDA, ROS and $Fe^{2+}$ contents. The ferroptosis-related proteins, such as SLC7A11, GPX4, TFR1, ACSL4, and FTH1, were examined using immunofluorescence and western blotting. Nrf2 was knocked down using siRNA to explore the molecular mechanism through which curcumin protects chondrocytes from erastin-induced ferroptosis. In a mouse model of knee ferroptosis induced by intracavity injection of 10 μL erastin (5 mg/mL), HE staining, Safranin O-Fast Green staining, and immunohistochemistry were employed to evaluate articular cartilage injury. The results demonstrated that erastin significantly suppressed the expression of SOD, GSH-PX, SLC7A11, GPX4, and FTH1 while upregulating the levels of LDH, MDA, ROS, ACSL4, and TFR1 in chondrocytes. Moreover, erastin-induced chondrocyte ferroptosis, lipid ROS, and $Fe^{2+}$ production were reversed by curcumin. Additionally, curcumin significantly upregulated the expression level of the Nrf2 gene and protein. Silencing Nrf2 reversed the protective effect of curcumin on erastin-induced chondrocyte ferroptosis. In animal experiments, silencing Nrf2 counteracted the impact and damage of curcumin on erastin-induced ferroptosis of cartilage tissue in vivo, leading to significant inhibition of OA progression. Taken together, these findings suggest that curcumin can inhibit chondrocyte ferroptosis by activating the Nrf2 signaling pathway, providing further insight into the regulatory mechanism of curcumin in OA and supporting its potential therapeutic use in OA treatment.

## 1. Introduction

Osteoarthritis (OA) is the most common degenerative joint disease, affecting 7% of the world's population and more than 500

* Corresponding author.
** Corresponding author.
*E-mail addresses:* zhouyizhao2020@Hunnu.edu.cn (Y. Zhou), 79986950@qq.com (Y. Zhou).

https://doi.org/10.1016/j.heliyon.2023.e20163
Received 17 January 2023; Received in revised form 25 August 2023; Accepted 13 September 2023
Available online 20 September 2023

million people [1]. It is characterized by the degeneration of articular cartilage, synovitis, and subchondral osteosclerosis. The incidence and prevalence of OA are on the rise due to factors such as an aging population, longer life expectancy, and increasing obesity [1,2]. Research has shown that the pathological death of chondrocytes is the primary cause of articular cartilage degeneration [3]. Therefore, alleviating articular cartilage degeneration by inhibiting chondroid death remains the focus of current research. However, no cell death inhibitors have been found to treat OA completely, suggesting that multiple forms of cell death may occur in OA and mediate the deterioration of cartilage inflammation [4].

Ferroptosis is a newly discovered form of cell death that plays a role in the pathogenesis of OA, and it is characterized by the accumulation of iron-dependent lipid peroxide, which reaches lethal levels [4]. Lipid peroxidation generates excessive reactive oxygen species (ROS), malondialdehyde (MDA), and peroxide dismutase (SOD), which can react with DNA or proteins to exert further toxic effects [5]. Glutathione peroxidase 4 (GPX4) is a lipid-repairing enzyme regulated by glutathione (GSH) that inhibits ferroptosis by reducing lipid peroxidation products and deadly ROS accumulation [6,7]. Inhibition of ferroptosis has been shown to effectively alleviate the development of OA [8,9]. It is noteworthy that nuclear factor erythroid 2-related factor 2 (Nrf2), a key antioxidant stress protein, can transcriptionally regulate ferroptosis-related proteins, including GPX4 and SLC7A11, which are involved in GSH synthesis [10,11]. System $Xc^-$ is a cysteine-glutamate reverse transporter that plays a crucial role in the GPX4 pathway of ferroptosis. Solute carrier family member 71 (SLC7A11), a specific subunit of system $Xc^-$, inhibits ferroptosis by promoting cystine uptake, GSH biosynthesis, and GPX4-mediated lipid peroxide detoxification [12]. Theaflavin-3,3′-digallate has been found to effectively inhibit erastin-induced ferroptosis in OA by activating Nrf2 signaling [13]. Nrf2 is also a significant target for omaveloxolone, which exerts antioxidant, anti-inflammatory, and anti-apoptotic effects on chondrocytes [14]. Therefore, the regulation of Nrf2 is crucial in combating OA and preventing cell death.

Curcumin, the main compound found in turmeric rhizomes, possesses various potential biological activities, such as anti-inflammatory, antioxidant, and antimicrobial properties, with minimal side effects [15]. It is considered to be one of the activators of Nrf2 [16]. Research has shown that curcumin combats conditions such as diabetic cardiomyopathy, cerebral hemorrhage and chronic obstructive pulmonary disease through its anti-ferroptosis properties [17,18]. Animal experiments have also demonstrated the therapeutic potential of curcumin in OA [19]. Clinical studies have confirmed its effectiveness in reducing knee injury, improving outcomes in OA, and relieving knee pain symptoms [20]. However, there is a lack of research on curcumin's regulation of ferroptosis in OA. As described by Miao et al. regulating a single mode of cell death may not be sufficient [4]. In addition to apoptosis and oxidative stress, it is plausible that curcumin may have other mechanisms by which it can treat OA.

Based on the above information, this study proposes that curcumin may inhibit ferroptosis in OA by targeting Nrf2. To investigate this, this study will construct OA cell models and mouse knee arthritis models through erastin and combine Nrf2 gene siRNA or shRNA to further explore curcumin's therapeutic mechanism.

## 2. Materials and methods

### 2.1. Isolation and identification of chondrocytes

All animal experiments in this study were approved by the Hunan Provincial People's Hospital Animal Experiment Ethics Committee (No. 202303). Four 4-week-old BALB/C mice (Shanghai JieSiJie Laboratory Animal Co., Ltd.) were euthanized using excess carbon dioxide. The knee cartilage was then dissected into small pieces and treated overnight at 37 °C with 0.1% collagenase type II. Chondrocytes were collected and cultured in DMEM (Gibco) supplemented with 10% fetal bovine serum (FBS, Gibco) in a thermostatic incubator at 5% CO2 and 37 °C. The expression levels of chondrocyte marker proteins, aggrecan (A11691, ABclonal) and collagen II (A19308, ABclonal), were assessed using immunofluorescence and western blotting after primary cell expansion culture.

### 2.2. CCK-8 cell viability assay

Cell viability was measured using the Cell Counting Kit-8 (CCK-8, Beyotime, Shanghai, China). Chondrocytes were inoculated into 96-well plates at a concentration of 5000 cells/well for 24 h and then treated with different concentrations of erastin (0, 0.37, 1.11, 3.33, 10, 30, 90 μM, Macklin, Shanghai, China) for 48 h. DMEM containing 10% CCK-8 solution was added to each well and incubated for 2 h, and the absorbance values were determined at 490 nm using a microplate reader (CMax Plus, Molecular Devices).

### 2.3. Drug selection

Curcumin, pterocarpin, ralenolide, resveratrol, psoralen chalcone, luteolin, daidzein, hydroxysafflor yellow A, geniposide, tetramethylpyrazine, astragaloside, genistein, and ferrostatin-1 (all from Zhejiang Ruyao Biotech Co., Ltd) were utilized in this study to screen for their anti-ferroptosis activity. Chondrocytes were seeded into 96-well plates at a concentration of 5000 cells/well and treated with 3 μM erastin for 24 h. They were then incubated with 5 μM of the aforementioned compounds separately added for an additional 48 h. Cell viability was subsequently evaluated using the CCK-8 assay. The control group did not receive any treatment with the test compounds. Furthermore, the cell activity was also assayed after the chondrocytes were cultivated with 3.33 μM erastin, followed by separate treatment with various concentrations (0, 0.5, 1, 2, 4, 8, 16, and 32 μM) of curcumin.

### 2.4. LDH content

Chondrocytes ($1 \times 10^6$) were exposed to 3.33 μM erastin and were treated with 0, 0.5, 2, or 8 μM curcumin for 48 h, respectively. The control group was not treated with any test compounds. After incubation, the supernatant was collected by centrifugation at 1000×*g* for 5 min, and the lactate dehydrogenase (LDH) content was measured by an LDH cytotoxicity assay kit (cat no. C0016, Beyotime, Shanghai, China).

### 2.5. Detection of oxidative stress indicators

Chondrocytes ($1 \times 10^6$) were exposed to 3.33 μM erastin and treated with 0, 0.5, 2, or 8 μM curcumin for 48 h, respectively. The levels of SOD (S0101S), glutathione peroxidase (GSH-Px, S0058) and MDA (S0131S) were measured using the corresponding assay kits purchased from Beyotime Biotechnology Co.

### 2.6. Detection of iron ion level

The iron ion content in cells was measured using the Iron Colorimetric Assay Kit (cat no. #K390-100, BioVision, Inc.). The absorbance values were evaluated at 593 nm using a microplate reader.

### 2.7. Detection of ROS

Chondrocytes ($1 \times 10^6$) were exposed to 3.33 μM erastin and treated with 0, 0.5, 2, or 8 μM curcumin separately for 48 h. After treatment, the cells were centrifuged at 2000 rpm for 5 min, the supernatant was discarded. And the cell pellet was then resuspended in PBS containing 5 μM DCFH-DA for 30 min at room temperature in the dark. Subsequently, the cells were washed twice with PBS and resuspended in 500 μL PBS. The levels of ROS in the cell suspensions were then detected by flow cytometry (Attune NxT, Thermo Fisher). Data acquisition and analysis were performed using FlowJo_V10 software (BD Biosciences, San Jose, CA, USA).

### 2.8. Immunofluorescence

Chondrocytes were exposed to 3.33 μM erastin and treated with 0, 0.5, 2, or 8 μM curcumin in 6-well plates containing coverslips for 48 h. After the treatment, the cells were fixed with 4% paraformaldehyde for 15 min, permeabilized with 0.5% Triton X-100 for 10 min and blocked with 1% BSA for 30 min at room temperature. The treated cells were incubated with primary antibodies against GPX4 (ab125066, Abcam), SLC7A11 (ab216876, Abcam) and ACSL4 (ab155282, Abcam) at 4 °C overnight. After overnight incubation, the cells were incubated with a FITC-labelled goat anti-rabbit (ab6717, Abcam) for 1 h in the dark. After washing 3 times with PBS, the cells were incubated with DAPI for 10 min to stain the nuclei. Images of the cells were captured using a fluorescence microscope (DM500, Leica). Image results were analyzed by Image-Pro Plus 6.0.

### 2.9. Western blot

The treated cells were lysed with 100 μL of RIPA lysis buffer containing a 1% protease inhibitor mixture for 30 min on ice and then denatured by boiling for 10 min. Proteins were electrophoresed in SDS–PAGE gels and then transferred to PVDF membranes (Millipore, USA). After being blocked with 5% skim milk, the membranes were incubated with primary antibodies [ACSL4, SLC7A11, GPX4, ferritin heavy chain (FTH1, ab183781, Abcam), transferrin receptor 1 (TFR1, ab214039, Abcam) and β-actin (ab213262, Abcam)] overnight at 4 °C. After three washes with TBST, the strips were incubated with secondary antibodies for 2 h at room temperature. Protein strips were developed and photographed by exposure using a chemiluminescent substrate kit (Boster, China) and a UVP imager (ChemiDoc-It Imaging System, UVP, USA). The optical density values of each strip were quantified by Image J.

### 2.10. RT–qPCR

Two micrograms of mRNA were extracted using the TRIzol method and reverse-transcribed into cDNA using the 1st Strand cDNA Synthesis Kit gDNA Purge Kit (E042, Novoprotein, China). qPCR was performed using the SYBR qPCR SuperMix Plus (E096, Novoprotein) kit in the 7500 Fast Real-Time PCR System (Applied Biosystems; Thermo Fisher Scientific, Inc.). The program was as follows: denaturation at 95 °C for 2 min; 10 s denaturation at 95 °C and annealing at 60 °C for 10 s, a total of 40 cycles; and extension at 72 °C for 30 s. The $2^{-\Delta\Delta Ct}$ method [21] was used to calculate the relative expression of the gene of interest. Amplification primers were designed through the NCBI online website in the following sequence:

Nrf2 Forwards: 5′-CAG CAT AGA GCA GGA CAT GGA G-3′, Nrf2 Reverse: 5′-GAA CAG CGG TAG TAT CAG CCA G-3’; β-actin Forwards: 5′- CAT TGC TGA CAG GAT GCA GAA GG-3′, β-actin Reverse: 5′- TGC TGG AAG GTG GAC AGT GAG G-3’.

### 2.11. Receptive research

Chondrocytes were transfected with 100 pmol Nrf2-siRNA oligonucleotide sequence using Lipofectamine RNAiMAX. The transfection efficiency was assessed by Western blot at 48 h posttransfection. The effects of 3.33 μM erastin, 8 μM curcumin, and Nrf2 siRNA

on cell activity, $Fe^{2+}$ accumulation levels, and expression of ferroptosis-related proteins were further examined. The Nrf2-siRNA primer sequences were designed by the online design software siDirect version 2.0 (http://sidirect2.rnai.jp/). The primers were as follows: Forwards: 5′- UAU UAA GAC ACU GUA AUU CGG-3′, Reverse: 5′- GAA UUA CAG UGU CUU AAU ACC-3'.

### 2.12. Nrf2-silenced lentivirus construction

We designed a mouse Nrf2 shRNA using the GPP Web Portal online website. Two complementary single-stranded oligonucleotides containing the target sequence were chemically synthesized and annealed. The double-stranded oligonucleotides were inserted between the *Age*I and *Eco*RI enzymatic cleavage sites of the pLKO.1-EGFP-puro plasmid. The ligated plasmids were transformed into *E. coli* DH5α cells for plasmid amplification and subsequently verified by DNA sequencing.

For transfection, a mixture of the recombinant plasmid, △△8.91 and pVSV-G (10: 10: 1) was transfected into 293T cells using the cationic lipid complex method (X-tremeGENE HP DNA transfection reagent, Roche). After 24 h, the cell cultures were collected and concentrated using a virus concentration kit (C2901 M, Beyotime). The final virus concentration was adjusted to $2 \times 10^{10}$ Vector Genomes/mL. shRNA primer sequences: Forwards Oligo 5′-CCG GAG GCA GCC ATG ACT GAT TTA ACT CGA GTT AAA TCA GTC ATG GCT GCC TTT TTT G-3′, Reverse Oligo: 5′-AAT TCA AAA AGC AGG CAT GAC TGA TTT AAC TCG AGT TAA ATC AGT CAT GGC TGC CT-3'.

### 2.13. Animal experiments

Thirty-two 8-week-old male BALB/C mice (adjusted appropriately according to the actual situation [22]) were anesthetized by intraperitoneal injection of pentobarbital (35 mg/kg). The mice were randomly divided into 4 groups (n = 6 per group): 1. Sham group, 10 μL 0.9% NaCl containing 10% cyclodextrin was injected intra-articularly into the left knee cavity; 2. Erastin group, 10 μL 5 mg/mL erastin was injected intra-articularly into the left knee cavity (prepared with 0.9% NaCl containing 10% cyclodextrin); 3. Erastin + Cur group, 10 μL of 5 mg/mL erastin was injected into the left knee cavity, and 50 mg/kg (= Human dose 3.56 mg/kg) [23, 24] curcumin (dissolved in corn oil) was given orally daily; 4. In the erastin + Cur + shNrf2 group, 10 μL of $2 \times 10^{10}$ VG/mL shNrf2

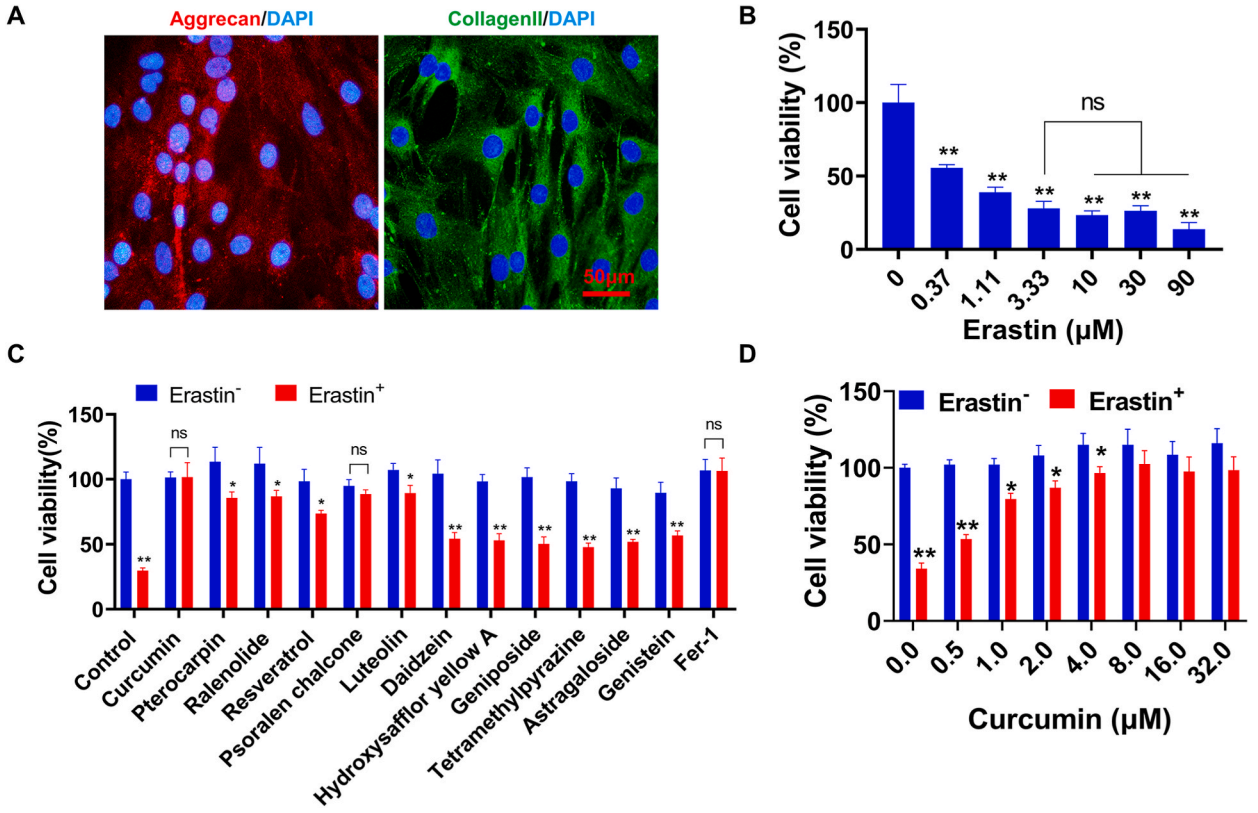


**Fig. 1.** Effect of curcumin on erastin-induced chondrocyte activity in mice (A) Immunofluorescence assessment of aggrecan and collagen II, chondrocyte signature proteins, for their expression and distribution in the normal group; (B) CCK-8 assay to determine the impact of different doses of erastin on chondrocyte cell viability; (C) CCK-8 assay to evaluate the effect of individual herbal monomers on erastin-induced chondrocyte cell viability; (D) CCK-8 assay to investigate the effect of varying doses of curcumin on erastin-induced chondrocyte cell viability. ($Erastin^-$ means no erastin added, $Erastin^+$ means 3.33 μM erastin added), $^{**}P < 0.01$, $^{*}P < 0.05$, the differences are statistically significant.

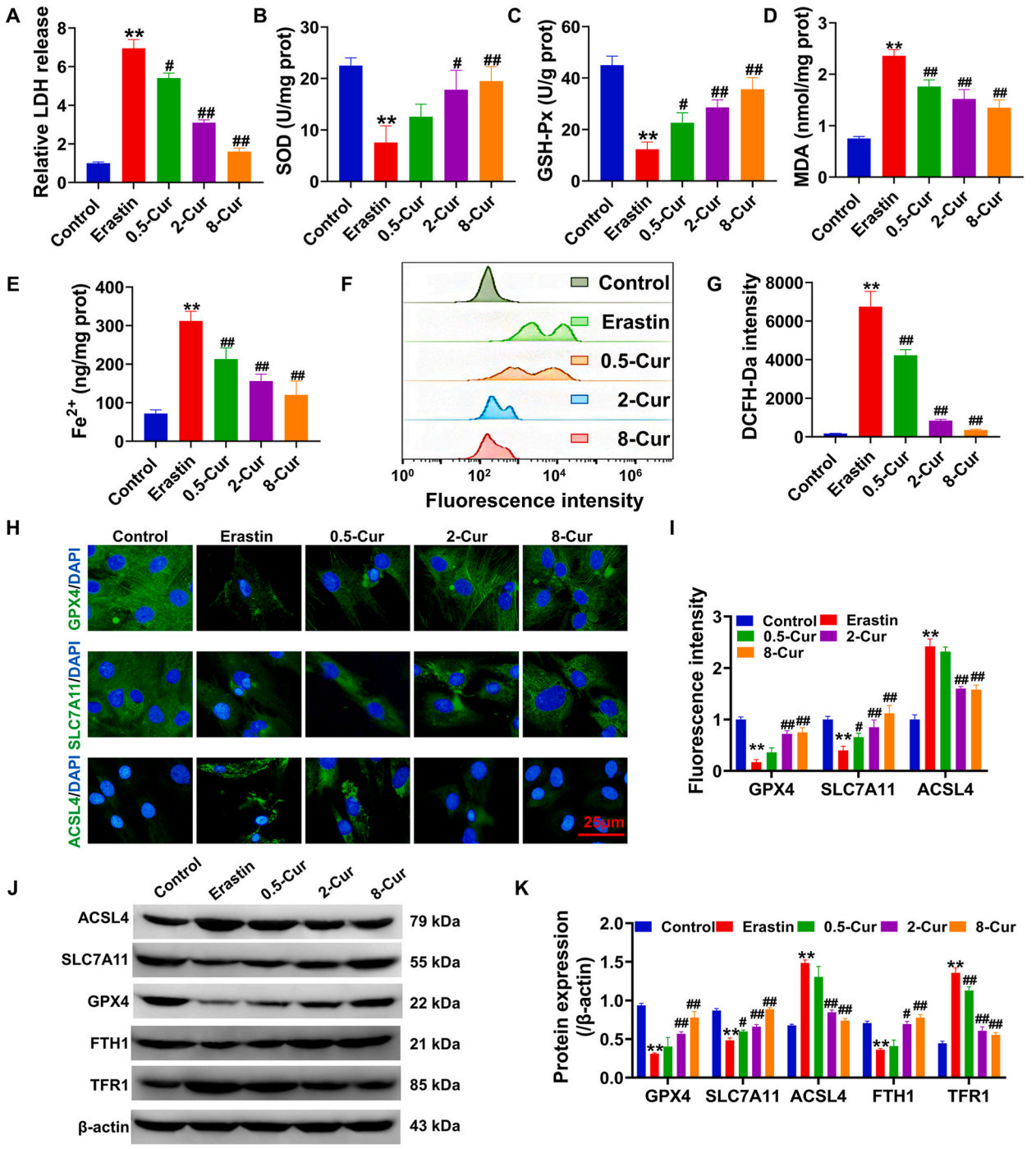


**Fig. 2.** Curcumin provides protection against erastin-induced ferroptosis in chondrocytes (A) LDH content assay; (B–E) Biochemical assay of SOD, GSH-Px, MDA, and $Fe^{2+}$ content; (F–G) Flow cytometry assay of intracellular ROS content by DCFH-Da probe method and data analysis using FlowJo V10; (H–I) Immunofluorescence assay of GPX4, SLC7A11 and ACSL4 protein expression levels and quantification by IPP 6.0 for quantitative statistics; (J–K) Western blot for expression levels of cellular ferroptosis -related proteins GPX4, SLC7A11, ACSL4, FTH1 and TFR1, and quantitative statistics for band optical density values. (Control group was not treated with any test compounds, Erastin group was treated with 3.33 μM erastin, 0.5, 2, and 8-Cur groups was treated with 3.33 μM erastin +0.5, 2, or 8 μM curcumin), **P < 0.01, *P < 0.05, compared with the control group; ##P < 0.01, #P < 0.05, compared with the erastin group.

lentivirus was injected into the left knee cavity once, followed by 10 μL of 5 mg/mL erastin the next day, and then 50 mg/kg curcumin was given orally every day. Erastin was injected every other day, and shNrf2 lentivirus was injected once every 4 weeks. The entire experiment lasted for 8 weeks. After euthanizing the mice, a portion of the knee joint was fixed in 4% paraformaldehyde for 24 h for pathological testing. Another part of the knee joint was used for western blotting to detect the expression levels of collagen II, Aggrecan, MMP-9, MMP-3, ACSL4, SLC7A11, GPX4, FTH1, TFR1, and Nrf2 proteins.

### 2.14. Histological assessment

The knee joints of the euthanized mice were fixed in 10% formalin at 4 °C for 24 h. Decalcification was performed at 4 °C using a saturated EDTA-$Na_2$ solution. After complete decalcification, the tissues were dehydrated in paraffin. Paraffin sections (5 μm) were

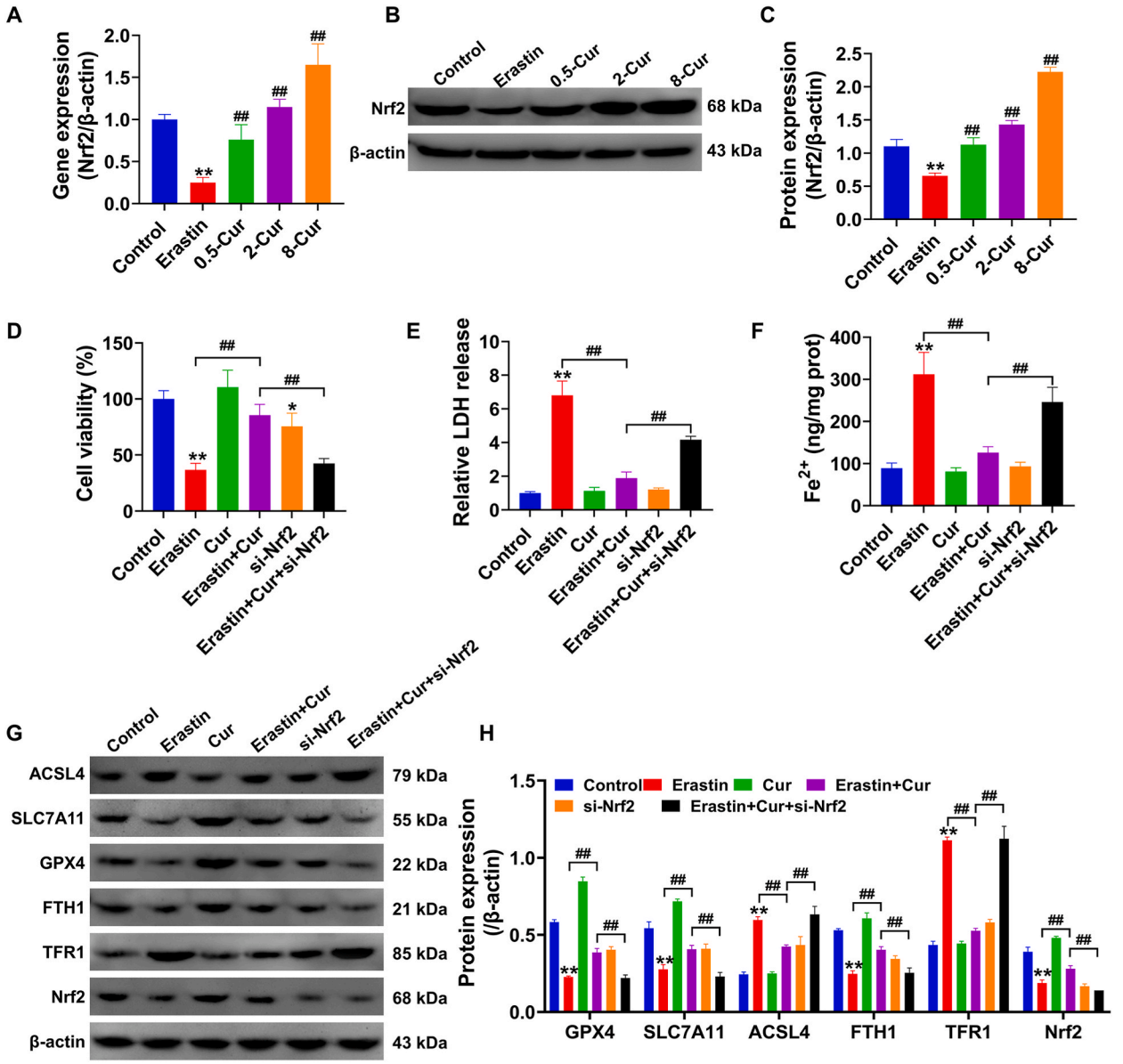


**Fig. 3.** Curcumin reverses erastin-induced ferroptosis in chondrocytes via Nrf2 (A) qPCR for cellular Nrf2 gene expression level; (B–C) Western blot for Nrf2 protein expression level and quantification of band optical density values; (D) CCK-8 for cellular activity level; **P < 0.01, *P < 0.05, compared with the control group; ##P < 0.01, #P < 0.05, compared with the erastin group. (E) LDH content of extracellular medium; (F) Intracellular $Fe^{2+}$ content; (G–H) Western blot for ACSL4, SLC7A11, GPX4, FTH1, TFR1 and Nrf2 protein expression levels and the optical density values of the bands were quantified and counted. **P < 0.01, *P < 0.05, compared with the control group; ##P < 0.01, #P < 0.05, linked groups for comparison.

stained with hematoxylin and eosin (H&E). Saffron O-solid green staining was used to stain the cartilage and mineralized bone of the bone tissues, with red indicating cartilage tissues, and green indicating mineralized bone tissue sites. In addition, immunohistochemical (IHC) staining of the bone tissues was also performed to detect the distribution and expression of aggrecan and collagen II proteins in bone tissues, following the protocol described in Ref. [24]. The experimental results were observed using light microscopy (DM500, Leica). The IHC results were quantified and analyzed using Image-Pro Plus 6 software.

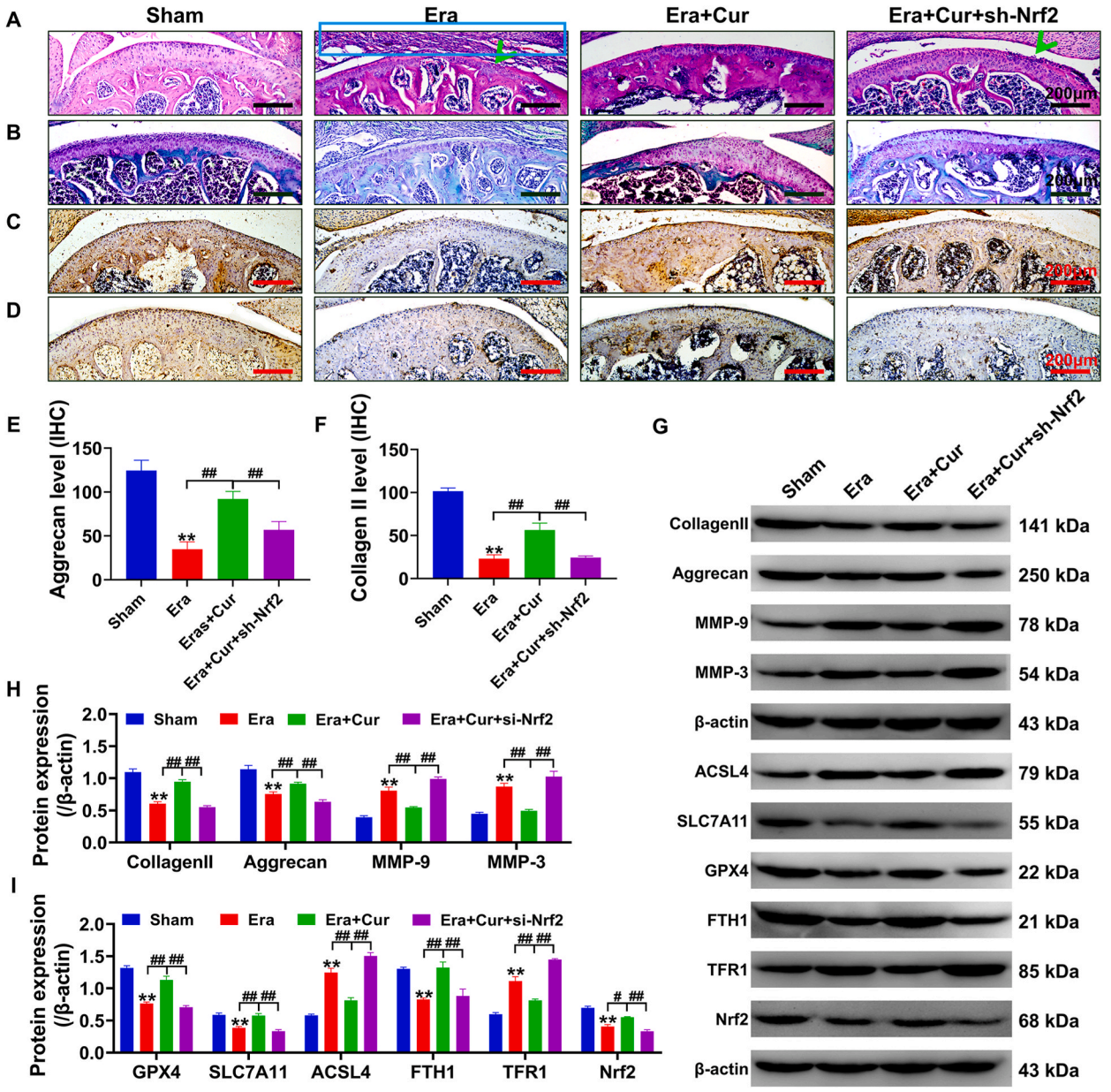


**Fig. 4.** Silencing of Nrf2 reverses the resistance of curcumin to erastin-induced ferroptosis in the knee joint of mice (A) HE staining for histopathological changes in the knee joint, blue boxes indicate proliferating synovial fibroblastic tissue, green arrows represent cartilage matrix loss and destruction sites; (B) Staining for cartilage (red) and osteogenic tissue (green) by guanine O-bright green; (C) IHC for aggrecan protein expression and distribution; (D) IHC for collagen II protein expression and distribution; (E–F) Quantification of aggrecan and collagen II protein IHC assay results; (G) Western blot was performed to detect the expression levels of collagen II, aggrecan, SLC7A11, GPX4, FTH1, Nrf2, MMP-9, MMP-3, ACSL4, and TFR1; (H–I) Quantification of the optical density values of the protein bands detected by Western blot. **P < 0.01, *P < 0.05, compared with the sham group; ##P < 0.01, #P < 0.05, linked groups for comparison. The scale bar in the figure is 200 μm.

### 2.15. Statistics analysis

The results are expressed as the mean ± standard deviation. Significance was determined using Student's *t*-test at a significance level of $p < 0.05$. Graphical representations of the experimental data were created using GraphPad Prism Software (version Prism 8; GraphPad Software, Inc.). Cellular experiments were conducted in triplicate as biological replicates. In the animal experimental, 3 mice per group were used for pathology-related experiments, and the other 3 were used for Western blot assays.

## 3. Results

### 3.1. Curcumin reverses the inhibitory effect of erastin on chondrocyte activity in mice

The IHC results (Fig. 1A) demonstrated positive expression of collagen II and aggrecan (chondrocyte marker protein) in primary mouse chondrocytes. Treatment with erastin significantly inhibited chondrocyte activity in a dose-dependent manner at 0.37–90 μM (Fig. 1B, $P < 0.01$). There were no significant changes observed in the inhibition of chondrocyte activity at concentrations of 3.33, 10, 30, and 90 μM erastin. Therefore, a concentration of 3.33 μM erastin was used for subsequent study. Furthermore, we investigated the effect of 5 μM herbal monomers on erastin-induced chondrocyte activity, and found that curcumin could reverse the inhibitory effects of erastin on chondrocyte activity (Fig. 1C). However, no significant differences in chondrocyte activity levels were observed between the control group and the erastin-induced group after treatment with 8, 16, and 32 μM curcumin for 48 h (Fig. 1D, $P > 0.05$).

### 3.2. Curcumin reduces the incidence of erastin-induced ferroptosis in chondrocytes

As the results of ferroptosis-related indicators showed (Fig. 2A–E), erastin significantly upregulated LDH secretion, intracellular MDA and $Fe^{2+}$ accumulation ($P < 0.01$) and inhibited the activity of SOD and GSH-Px enzyme in chondrocytes compared with the control group ($P < 0.01$). Treatment with 2 and 8 μM curcumin significantly reduced LDH, MDA, and $Fe^{2+}$ contents ($P < 0.01$), and increased SOD and GSH-Px enzyme activities, with statistically significant differences compared to the erastin group ($P < 0.05$). Additionally, 0.5, 2, and 8 μM curcumin significantly inhibited the accumulation of ROS in the cells, with statistically significant compared with the erastin group ($P < 0.01$, Fig. 2F–G). Immunofluorescence assay results (Fig. 2H–I) showed that both 2 and 8 μM curcumin significantly suppressed the expression of ACSL4 protein and enhanced the expression intensity of GPX4 and SLC7A11 proteins ($P < 0.01$ compared with the erastin group, Fig. 2H–I). Furthermore, 2 and 8 μM curcumin promoted the expression of the anti-ferroptosis proteins GPX4, SLC7A11, and FTH1, leading to significant inhibition of the expression levels of the pro-ferroptosis proteins ACSL4 and TFR1 ($P < 0.01$ compared with the erastin group, Fig. 2J–K).

### 3.3. Curcumin inhibits erastin-induced ferroptosis via Nrf2

We further investigated whether curcumin reverses erastin-induced ferroptosis in chondrocytes through the Nrf2 pathway, which is a classical target of curcumin known. The results demonstrated that treatment with 0.5, 2, and 8 μM curcumin significantly upregulated the expression levels of the Nrf2 gene and protein (Fig. 3A–C), with statistically significant compared with the erastin group ($P < 0.01$). Nrf2 siRNA significantly reversed the upregulation of chondrocyte activity (erastin-induced) by 8 μM curcumin (Fig. 3D), with a statistically significant compared to the erastin + cur group ($P < 0.01$). Moreover, the erastin + cur + si-Nrf2 group showed significantly inhibited LDH and $Fe^{2+}$ levels, with statistically significant differences compared to the erastin + cur group ($P < 0.01$, Fig. 3E–F). Western blot results (Fig. 3G–H) revealed that the erastin + cur + si-Nrf2 group effectively suppressed the expression of GPX4, SLC7A11, FTH1, and Nrf2 proteins, while upregulating the expression levels of ACSL4 and TFR1 proteins, with statistically significant difference compared to the erastin + cur group ($P < 0.01$).

### 3.4. Silencing of Nrf2 reverses the resistance of curcumin to erastin-induced ferroptosis in the knee joint of mice

We induced arthritis in mice with erastin. In the Era model group, erastin caused erosion of cartilage tissue and loss of cartilage matrix in the knee joints of mice (shown by green arrows), treatment with curcumin alleviated the damage caused by erastin (Fig. 4A–B). Additionally, erastin promoted the proliferation of synovial fibroblastic tissue (blue boxed site) (Fig. 4A). However, no significant pathological structural changes were observed in the Era + Cur group. In contrast, the Era + Cur + sh-Nrf2 group, in which Nrf2 was silenced, exhibited the loss of aggrecan (Fig. 4C) and collagen II (Fig. 4D) in the knee joint of Era group mice was severe (red positive reaction), leading to cartilage tissue damage. This indicates that sh-Nrf2 reversed the upregulation of aggrecan and collagen II in the Era + Cur group ($P < 0.01$). Western blot analysis revealed significant upregulation of collagen II, aggrecan, SLC7A11, GPX4, FTH1, and Nrf2, while the expression levels of MMP-9, MMP-3, ACSL4, and TFR1 were significantly suppressed in the Era + Cur group (Fig. 4G–I, $P < 0.05$, compared with the Era group). However, silencing Nrf2 effectively reversed the treatment effect of curcumin ($P < 0.01$, compared with the Era + Cur + sh-Nrf2 group).

## 4. Discussion

Erastin was first identified in 2003 as a compound that induces ferroptosis, which was used for screening cancer drugs that selectively kill oncogenic RAS mutant cell lines [25]. It functions by inhibiting SLC7A11, a membrane transporter that imports cystine

into the cell for the synthesis of the antioxidant glutathione (GSH) [26]. By inhibiting SLC7A11, erastin depletes intracellular GSH and inactivates the enzyme glutathione peroxidase 4 (GPX4), resulting in increased lipid ROS formation and peroxidation, ultimately leading to ferroptosis [27]. In this study, we used erastin to induce ferroptosis in mouse chondrocytes to mimic the pathophysiology of OA. We observed the downregulation of the proteins SLC7A11, GPX4, and FTH1 (ferroptosis-inhibiting protein) in erastin-treated chondrocytes. Conversely, the expression of ACSL4 and TFR1 (ferroptosis-promoting protein) was upregulated, which is consistent with previous studies [9]. Oxidative stress is known to be elevated in OA cartilage and is a major contributor to chronic inflammation [28]. Curcumin has been demonstrated to possess antioxidative stress and ferroptosis-inhibiting properties [17]. In this study, we discovered that curcumin has the ability to effectively reverse the inhibitory effects of erastin on chondrocyte activity. At first, the evidence of LDH level restoration suggests that curcumin can effectively alleviate cell damage [29]. Further comprehensive investigations have provided additional support for the inhibitory effects of curcumin on the accumulation of MDA and ROS, which are indicators of oxidative stress damage. In addition, curcumin enhances the activities of SOD and GSH-Px enzymes, which serve as indicators of antioxidative stress in chondrocytes. By reducing ROS production and lipid peroxidation, curcumin effectively mitigates the oxidative stress damage caused by ferroptosis [30]. Furthermore, curcumin upregulates the expression of SLC7A11, GPX4, and FTH1 proteins, this leads to a reduction in $Fe^{2+}$ accumulation in chondrocytes and significantly reverses erastin-induced ferroptosis. The SLC7A11-GSH-GPX4 axis constitutes one of the defense systems against ferroptosis, and the increased expression of SLC7A11 and GPX4 proves beneficial in inhibiting lipid peroxidation induced by ferroptosis [31]. Moreover, FTH1 plays a role in the efficient uptake and recycling of iron while reducing levels of free iron ions [31]. Overall, these findings suggest that curcumin can effectively inhibit the progression of ferroptosis.

Nrf2 is not only a primary antioxidant system in cells but also a critical protective factor in mitigating ferroptosis [22]. Numerous studies have demonstrated that activating Nrf2 can alleviate OA [1,32–35], making it an attractive target for OA ferroptosis [13]. The present study confirmed that curcumin, used in the treatment of OA, significantly activates Nrf2 [17,18]. To further elucidate the mechanism of ferroptosis in OA treated with curcumin, Nrf2 siRNA was used for the reversibility study. The results demonstrated that interfering with the gene and protein expression levels of Nrf2 significantly weakened the protective effect of curcumin to erastin-induced ferroptosis and attenuated the resistance of chondrocytes to oxidative stress.

To further investigate whether the protective effects of curcumin against ferroptosis in OA occur through Nrf2 activation in vivo, we induced ferroptosis in mouse knee joints using erastin and silenced Nrf2 at mouse knee joint sites using lentivirus. Safranin O and HE staining demonstrated that curcumin attenuated cartilage degeneration and significantly alleviated erastin-induced cartilage erosion and matrix loss. Furthermore, curcumin upregulated the expression of aggrecan and collagen II proteins in knee joint tissues. It also inhibited the expression of MMP-9 and MMP-3 proteins, which helped maintain the physiological and biomechanical properties of articular cartilage [19,36]. Western blot analysis further revealed that curcumin significantly increased the expression levels of the anti-ferroptosis-related proteins SLC7A11, GPX4, and FTH1, while inhibiting the expression of pro-ferroptosis-related proteins. Importantly, the silencing of the Nrf2 gene reversed all of these effects observed with curcumin. Therefore, these findings suggest that curcumin enhances the ferroptosis resistance of chondrocytes by activating Nrf2.

Some limitations of this study should be acknowledged. Firstly, the standard gold standard method for detecting ferroptosis has not been established, unlike apoptosis. However, we verified that erastin induces chondrocyte ferroptosis based on the definition of ferroptosis by the cell death nomenclature committee. Moreover, we provided preliminary evidence suggesting that curcumin may inhibit chondrocyte ferroptosis and delay the OA progression in vivo and in vitro. Secondly, the animal model used in this study was not a classical OA animal model but rather a knee joint ferroptosis model induced by erastin. While this is sufficient to demonstrate the effectiveness of curcumin in preventing ferroptosis in cartilage joints, further validation using classical OA-related models would be beneficial.

Our findings provide confirmation that curcumin has the potential to protect against OA both in vitro and in vivo through the activation of the Nrf2 pathway. Additionally, we demonstrated that curcumin effectively mitigates chondrocyte ferroptosis, thereby reducing the loss of collagen and glycoprotein in cartilage tissues, as observed in erastin-treated chondrocytes and knee joints. This study contributes to our understanding of the mechanism by which curcumin treats OA by regulating ferroptosis and provides a stronger theoretical basis for the clinical use and treatment of curcumin. However, there are some limitations to this study as it was only conducted on mice, and further validation is needed in human cells in the future.

## Author contribution statement

Yizhao Zhou; Zhen Jia: Conceived and designed the experiments; Performed the experiments; Wrote the paper.
Jing Wang; Shu Huang; Shu Yang: Performed the experiments.
Sheng Xiao; Duo Xia; Yi Zhou: Analyzed and interpreted the data; Contributed reagents, materials, analysis tools or data.

## Availability of data and materials

This study's data can be obtained from the corresponding author upon reasonable request.

## Funding

This work was supported by the Project of Hunan Provincial Department of Education (NO·20C1149) and Natural Science Foundation of Hunan Province (NO.2021JJ304060).

## Declaration of competing interest

The authors declare that they have no known competing financial interests or personal relationships that could have appeared to influence the work reported in this paper.

## References


[1] D.J. Hunter, L. March, M. Chew, Osteoarthritis in 2020 and beyond: a lancet commission, Lancet 396 (10264) (2020) 1711–1712.
[2] D.J. Hunter, S. Bierma-Zeinstra, Osteoarthritis, Lancet 393 (10182) (2019) 1745–1759.
[3] I. Morales-Ivorra, M. Romera-Baures, B. Roman-Viñas, L. Serra-Majem, Osteoarthritis and the mediterranean diet: a systematic review, Nutrients 10 (8) (2018).
[4] Y. Miao, Y. Chen, F. Xue, K. Liu, B. Zhu, J. Gao, J. Yin, C. Zhang, G. Li, Contribution of ferroptosis and GPX4's dual functions to osteoarthritis progression, EBioMedicine 76 (2022), 103847.
[5] M.M. Gaschler, B.R. Stockwell, Lipid peroxidation in cell death, Biochem. Biophys. Res. Commun. 482 (3) (2017) 419–425.
[6] S. Wei, T. Qiu, X. Yao, N. Wang, L. Jiang, X. Jia, Y. Tao, Z. Wang, P. Pei, J. Zhang, Y. Zhu, G. Yang, X. Liu, S. Liu, X. Sun, Arsenic induces pancreatic dysfunction and ferroptosis via mitochondrial ROS-autophagy-lysosomal pathway, J. Hazard Mater. 384 (2020), 121390.
[7] F. Ursini, M. Maiorino, Lipid peroxidation and ferroptosis: the role of GSH and GPx4, Free Radic. Biol. Med. 152 (2020) 175–185.
[8] S. Wang, W. Li, P. Zhang, Z. Wang, X. Ma, C. Liu, K. Vasilev, L. Zhang, X. Zhou, L. Liu, J. Hayball, S. Dong, Y. Li, Y. Gao, L. Cheng, Y. Zhao, Mechanical overloading induces GPX4-regulated chondrocyte ferroptosis in osteoarthritis via Piezo1 channel facilitated calcium influx, J. Adv. Res. 41 (2022) 63–75.
[9] J. Yan, G. Feng, L. Ma, Z. Chen, Q. Jin, Metformin alleviates osteoarthritis in mice by inhibiting chondrocyte ferroptosis and improving subchondral osteosclerosis and angiogenesis, J. Orthop. Surg. Res. 17 (1) (2022) 333.
[10] Z. Qiang, H. Dong, Y. Xia, D. Chai, R. Hu, H. Jiang, Nrf2 and STAT3 alleviates ferroptosis-mediated IIR-ALI by regulating SLC7A11, Oxid. Med. Cell. Longev. 2020 (2020), 5146982.
[11] T. Kose, P.A. Sharp, G.O. Latunde-Dada, Upregulation of Nrf2 signalling and the inhibition of erastin-induced ferroptosis by ferulic acid in MIN6 cells, Int. J. Mol. Sci. 23 (24) (2022).
[12] P. Koppula, L. Zhuang, B. Gan, Cystine transporter SLC7A11/xCT in cancer: ferroptosis, nutrient dependency, and cancer therapy, Protein Cell 12 (8) (2021) 599–620.
[13] C. Xu, S. Ni, N. Xu, G. Yin, Y. Yu, B. Zhou, G. Zhao, L. Wang, R. Zhu, S. Jiang, Y. Wang, Theaflavin-3,3'-Digallate inhibits erastin-induced chondrocytes ferroptosis via the nrf2/GPX4 signaling pathway in osteoarthritis, Oxid. Med. Cell. Longev. 2022 (2022), 3531995.
[14] Z. Jiang, G. Qi, W. Lu, H. Wang, D. Li, W. Chen, L. Ding, X. Yang, H. Yuan, Q. Zeng, Omaveloxolone inhibits IL-1β-induced chondrocyte apoptosis through the Nrf2/ARE and NF-κB signalling pathways in vitro and attenuates osteoarthritis in vivo, Front. Pharmacol. 13 (2022), 952950.
[15] S.G. Ibrahim, S.Z. El-Emam, E.A. Mohamed, M.F. Abd Ellah, Dimethyl fumarate and curcumin attenuate hepatic ischemia/reperfusion injury via Nrf2/HO-1 activation and anti-inflammatory properties, Int. Immunopharm. 80 (2020), 106131.
[16] X. Zhang, Y. Cui, X. Song, X. Jin, X. Sheng, X. Xu, T. Li, H. Chen, L. Gao, Curcumin alleviates ketamine-induced oxidative stress and apoptosis via Nrf2 signaling pathway in rats' cerebral cortex and hippocampus, Environ. Toxicol. 38 (2) (2023) 300–311.
[17] Z. Wei, Q. Shaohuan, K. Pinfang, S. Chao, Curcumin attenuates ferroptosis-induced myocardial injury in diabetic cardiomyopathy through the Nrf2 pathway, Cardiovasc Ther 2022 (2022), 3159717.
[18] C. Yang, M. Han, R. Li, L. Zhou, Y. Zhang, L. Duan, S. Su, M. Li, Q. Wang, T. Chen, Y. Mo, Curcumin nanoparticles inhibiting ferroptosis for the enhanced treatment of intracerebral hemorrhage, Int. J. Nanomed. 16 (2021) 8049–8065.
[19] C. Buhrmann, A. Brockmueller, A.L. Mueller, P. Shayan, M. Shakibaei, Curcumin attenuates environment-derived osteoarthritis by Sox9/NF-kB signaling Axis, Int. J. Mol. Sci. 22 (14) (2021).
[20] A.L. Lopresti, S.J. Smith, S. Jackson-Michel, T. Fairchild, An investigation into the effects of a curcumin extract (Curcugen®) on osteoarthritis pain of the knee: a randomised, double-blind, placebo-controlled study, Nutrients 14 (1) (2021).
[21] X. Rao, X. Huang, Z. Zhou, X. Lin, An improvement of the 2ˆ(-delta delta CT) method for quantitative real-time polymerase chain reaction data analysis, Biostatistics, bioinformatics and biomathematics 3 (3) (2013) 71–85.
[22] Z. Guo, J. Lin, K. Sun, J. Guo, X. Yao, G. Wang, L. Hou, J. Xu, J. Guo, F. Guo, Deferoxamine alleviates osteoarthritis by inhibiting chondrocyte ferroptosis and activating the Nrf2 pathway, Front. Pharmacol. 13 (2022), 791376.
[23] V. Sorrenti, G. Contarini, S. Sut, S. Dall'Acqua, F. Confortin, A. Pagetta, P. Giusti, M. Zusso, Curcumin prevents acute neuroinflammation and long-term memory impairment induced by systemic lipopolysaccharide in mice, Front. Pharmacol. 9 (2018) 183.
[24] R.R. Falah, W.H. Talib, S.J. Shbailat, Combination of metformin and curcumin targets breast cancer in mice by angiogenesis inhibition, immune system modulation and induction of p53 independent apoptosis, Ther Adv Med Oncol 9 (4) (2017) 235–252.
[25] S. Dolma, S.L. Lessnick, W.C. Hahn, B.R. Stockwell, Identification of genotype-selective antitumor agents using synthetic lethal chemical screening in engineered human tumor cells, Cancer Cell 3 (3) (2003) 285–296.
[26] R.J. Bridges, N.R. Natale, S.A. Patel, System xc⁻ cystine/glutamate antiporter: an update on molecular pharmacology and roles within the CNS, Br. J. Pharmacol. 165 (1) (2012) 20–34.
[27] G.C. Forcina, S.J. Dixon, GPX4 at the crossroads of lipid homeostasis and ferroptosis, Proteomics 19 (18) (2019), e1800311.
[28] M.Y. Ansari, N. Ahmad, T.M. Haqqi, Oxidative stress and inflammation in osteoarthritis pathogenesis: role of polyphenols, Biomed. Pharmacother. 129 (2020), 110452.
[29] L. Ni, C. Yuan, X. Wu, Targeting ferroptosis in acute kidney injury, Cell Death Dis. 13 (2) (2022) 182.
[30] S. Samarghandian, M. Azimi-Nezhad, T. Farkhondeh, F. Samini, Anti-oxidative effects of curcumin on immobilization-induced oxidative stress in rat brain, liver and kidney, Biomed. Pharmacother. 87 (2017) 223–229.
[31] Y. Wang, S. Wu, Q. Li, H. Sun, H. Wang, Pharmacological inhibition of ferroptosis as a therapeutic target for neurodegenerative diseases and strokes, Adv. Sci. (2023), e2300325.
[32] L. Wang, C. He, Nrf2-mediated anti-inflammatory polarization of macrophages as therapeutic targets for osteoarthritis, Front. Immunol. 13 (2022), 967193.
[33] N.M. Khan, I. Ahmad, T.M. Haqqi, Nrf2/ARE pathway attenuates oxidative and apoptotic response in human osteoarthritis chondrocytes by activating ERK1/2/ELK1-P70S6K-P90RSK signaling axis, Free Radic. Biol. Med. 116 (2018) 159–171.
[34] J.W. Li, R.L. Wang, J. Xu, K.Y. Sun, H.M. Jiang, Z.Y. Sun, Z.Y. Lv, X.Q. Xu, R. Wu, H. Guo, Q. Jiang, D.Q. Shi, Methylene blue prevents osteoarthritis progression and relieves pain in rats via upregulation of Nrf2/PRDX1, Acta Pharmacol. Sin. 43 (2) (2022) 417–428.
[35] Q. Zhang, X. Bai, R. Wang, H. Zhao, L. Wang, J. Liu, M. Li, Z. Chen, Z. Wang, L. Li, D. Wang, 4-octyl Itaconate inhibits lipopolysaccharide (LPS)-induced osteoarthritis via activating Nrf2 signalling pathway, J. Cell Mol. Med. 26 (5) (2022) 1515–1529.
[36] K. Ito, T. Shinomura, Development and application of a new Silent reporter system to quantitate the activity of enhancer elements in the type II Collagen Gene, Gene 585 (1) (2016) 13–21.